Title
Dual-layered hydrogels allow complete genome recovery with nucleic acid cytometry

Journal
Biotechnology Journal, 17(4)

ISSN
1860-6768

Authors
Hatori, Makiko N
Modavi, Cyrus
Xu, Peng
et al.

Publication Date
2022-04-01

DOI
10.1002/biot.202100483

Peer reviewed

Published in final edited form as:

Biotechnol J. 2022 April ; 17(4): e2100483. doi:10.1002/biot.202100483.

Dual-layered hydrogels allow complete genome recovery with nucleic acid cytometry

Makiko N. Hatori[1],

Cyrus Modavi[1],

Peng Xu[1],

Daniel Weisgerber[1],

Adam R. Abate[1,2]

[1]Department of Bioengineering and Therapeutic Sciences, California Institute for Quantitative Biosciences, University of California, San Francisco, California, USA

[2]Chan Zuckerberg Biohub, San Francisco, California, USA

Abstract

Targeting specific cells for sequencing is important for applications in cancer, microbiology, and infectious disease. Nucleic acid cytometry (NAC) is a powerful approach for accomplishing this because it allows specific cells to be isolated based on sequence biomarkers that are otherwise impossible to detect. However, existing methods require specialized microfluidic devices, limiting adoption. Here, a modified workflow is described that uses particle-templated emulsification (PTE) and flow cytometry to conduct the essential steps of cell detection and sorting normally accomplished by microfluidics. Our microfluidic-free workflow allows facile isolation and sequencing of cells, viruses, and nucleic acids and thus provides a powerful enrichment approach for targeted sequencing applications.

Keywords

enrichment; genomics; hydrogels; microfluidics; PCR; sequencing

1 | INTRODUCTION

A common need in single cell analysis is characterizing specific cells in large, heterogeneous populations. This arises when answering questions relating to sub-populations,[1–3] generating detailed atlases that should capture all relevant cell types,

Correspondence Adam R. Abate, UCSF – Mission Bay, 1700 4th, Street Byers Hall, Room 303C, San Francisco, CA 94158, USA. adam@abatelab.org.

CONFLICT OF INTEREST

The authors declare no conflicts of interest.

SUPPORTING INFORMATION

Additional supporting information may be found in the online version of the article at the publisher's website.

[4–6] or seeking to deeply characterize the genomic and phenotypic properties of rare cells.[7,8] In the absence of enrichment, such objectives require prohibitively expensive sequencing of uninteresting, abundant cell types. Common enrichment methods require pre-labeling cells with antibodies or oligos, then sorting with flow or magnetic cytometry.[9–13] However, often, specific surface markers are unavailable or unknown for antibody labeling,[14,15] while oligo hybridization methods have limited sensitivity.[11] Microfluidic droplet encapsulation with polymerase chain reaction (PCR) screening affords a unique and powerful approach for detecting specific cell types based on nucleic acid biomarkers and, when combined with active or inertial microfluidic sorting, affords superb enrichment of rare subpopulations.[16–22] This paradigm, called nucleic acid cytometry (NAC),[23] is capable of multiplexed DNA and RNA sequence detection,[18] can be integrated with conventional single-cell antibody staining methods,[13,24] and can isolate cells,[18,25] viral particles,[26] and DNA strands[27,28] from complex mixtures. The application of NAC has enabled the isolation of numerous cell types, viruses, and nucleic acids that would otherwise have been impossible to capture. However, a major barrier to implementing NAC is the requirement of microfluidics to encapsulate and sort the droplets;[23] these components are available only in specialized labs, preventing broad adoption of the approach. To facilitate adoption of NAC techniques, a new approach is needed that requires no specialized microfluidics and can be performed in common biological laboratories.

In this paper, we demonstrate a new NAC approach that requires no microfluidics, instead employing Particle-Templated Emulsification (PTE)[29] and Fluorescence-Activated Cell Sorting (FACS) to detect and sort cells. The core innovation enabling this microfluidic-free workflow is a dual-layered hydrogel particle consisting of a functionalized polyacrylamide core and agarose shell. The core captures fluorescent amplicons generated by PCR,[30] while the surrounding agarose captures the genomes of the cells. Post-thermocycling, particles carrying the target cells have fluorescent cores that can be sorted via FACS, allowing isolation and full genome sequencing of the captured microbe. This microfluidic-free approach allows facile recovery of organisms currently unsortable with FACS or other enrichment methods in a format accessible to non-microfluidic labs.

2 | EXPERIMENTAL SECTION

2.1 | Two layered beads preparation

A total 6.2% acrylamide (Sigma-Aldrich), 0.18% N,N’-Methylenebisacrylamide (Sigma-Aldrich), 0.3% ammonium persulphate (Sigma-Aldrich), and 4 mM of acrydite modified primer MH075 (IDT sequence: /5Acryd//iSpPC/ ATATTACTCTTTCCCTACACGACGCTCTTC) were used for PAA particle generation. The PAA solution and fluorinated oil supplemented with 1% Tetramethylethylenediamine (Sigma-Aldrich) were loaded into 1-ml syringes (BD) and injected into a bubble-trigger device.[31] The syringes were placed on syringe pumps (New Era, NE-501) and controlled with a custom Python script (https://github.com/AbateLab/Pump-Control-Program) to pump oil at 3500 $\mu l\ h^{-1}$ and PAA solution at 1300 $\mu l\ h^{-1}$. The PAA droplets were collected and incubated for 3 h at room temperature for gelation. To break the emulsion, the gelled droplets were transferred to an aqueous carrier by destabilizing them in oil with addition

of an equal volume of 20% v/v perfluoro-1-octanol in HFE-7500.[32] The particles were washed twice with hexane containing 2% Span-80 (Sigma-Aldrich) to remove residual oil. Following the hexane wash, the particles were washed with a Tris-Buffered Saline formulation (TBSTE: 20 mM Tris-HCl pH 8.0, 274 mM NaCl, 5.4 mM KCl, 0.2% Triton X-100, 20 mM EDTA) until all oil was removed. Prior to use, solidified PAA droplets were filtered using a 70 μm cell strainer (Corning Falcon Cell Strainer) to remove large beads and prevent device clogging. Droplets were packed in a syringe by centrifugation at 3500 rpm for 5 min using a custom 3D printed syringe adapter. Excess supernatant was subsequently removed. To make the agarose shell, packed PAA particles, 3.5% ultra-low gelling temperature agarose (Sigma-Aldrich) solution, and HFE-7500 fluorinated oil (3 M) with 2% w/w PEG-PFPE amphiphilic block copolymer surfactant (008-Fluoro-surfactant, Ran Technologies) were injected into the bubble trigger device respectively at 700, 1000, and 6000 $\mu l\ h^{-1}$. The droplets were collected and agarose solidification occured for 1 h on ice. The droplets awee broken as described and used for ddPCR.

Droplets were imaged using the EVOS Cell Imaging System (Thermo Fisher Scientific). Images were taken under a 4x and 10x objective using EVOS FITC LED light sources.

2.2 | Device fabrication

The microfluidic devices were fabricated from photoresist masters. The masters were made by spinning the SU-8 photoresist (Microchem) onto a 3-inch silicon wafer (University Wafer). The choice of SU-8 and spin speed was determined by the channel height of the microfluidic device. After baking at 95°C for 45 min, the photoresist on the wafer was exposed to ultraviolet light for 1 min over photolithography masks (CAD/Art Services) with patterns of microfluidic channels. The wafer was then baked at 95°C for 5 min, cooled to room temperature and then developed for 15 min in propylene glycol monomethyl ether acetate (PGMEA, Sigma Aldrich). After development, the wafer was then rinsed with fresh PGMEA and isopropanol, before being dried by blowing with air. After baking at 65°C for 1 h to remove solvent, the wafer with channel patterns was stored as the photoresist master.

The microfluidic devices were made by pouring a polydimethylsiloxane solution (PDMS, Dow Corning, Sylgard 184) with a 10:1 polymer-to-crosslinker ratio over the master and then cured at 65°C overnight. The devices were extracted with a metal scalpel, and punched with a 0.75 mm biopsy punch (World Precision Instruments, catalog no. 504529) to create holes at each fluid inlet or outlet. Devices were bonded to a glass slide after plasma treatment and the channels were made hydrophobic by treatment with Aquapel (PPG Industries).

2.3 | ddPCR

A total 1.2 million beads pre-washed with sterile water were suspended in 150 μl of sterile water and mixed with 350 μl of 2X Phire Plant PCR Buffer, 14 μl of Phire Hot Start II DNA Polymerase (Thermo Fisher Scientific), 0.816 M of 1,2-propanediol[33] (Sigma-Aldrich), and 500 nM of forward and reverse primers (IDT) targeting the PdeK gene. The primer sequences are as follows:

MH129 5′-
CTCTTTCCCTACACGACGCTCTTCAGCCAGACATGAAGCTGATAC-3′,

MH130 5′- /56-FAM/TGCACGCCGTCGAAATTA-3′.

The mixture was incubated for 15 min to allow PCR reagent to diffuse into the particles, and then centrifuged for 1 min at 6000 rpm. Excess aqueous phase was removed with a pipette. *Escherichia coli* cells were counted manually under a microscope and diluted as needed to an appropriate concentration for single-cell encapsulation. Particles, 12,000 *E. coli* cells, 200 μl of HFE-7500 oil supplemented with 5% w/w PFPE-PEG-PFPE surfactant (008-Fluoro-surfactant, RAN Biotechnologies), and enough Triton X-100 for a final concentration of 0.5% v/v were mixed well in a 1.7-ml Eppendorf tube by tapping. The mixture was agitated at 3500 rpm for 20 s with a vortex (VWR) to generate the emulsion. After transferring the emulsion to PCR tubes, the oil under the buoyant droplets was removed with a pipette and replaced with FC-40 oil (Sigma-Aldrich) containing 5%w/w PFPE-PEGPFPE surfactant. This oil and surfactant system provides greater emulsion stability during the thermocycling.[29,34] The emulsion was transferred to a T100 thermocycler (Bio-Rad) and subjected to the following program: 87°C for 5 min, followed by 35 cycles of 87°C for 5 s, 53°C for 5 s and 72°C for 20 s, followed by final extension of 1 min at 72°C and held at 4°C until processed. The droplets are imaged using the EVOS Cell Imaging System (Thermo Fisher Scientific) under a 10× and 20× objective with EVOS GFP and FITC LED light sources. After thermocycling, the emulsions were broken by adding 1H,1H,2H,2H-Perfluoro1-octanol (final concentration 20% v/v, Sigma-Aldrich) and mixing.[32] Recovered particles in the aqueous fraction were used for downstream sorting and processing.

2.4 | FACS

FACS analysis was performed on a FACS Aria II using a 130 μm nozzle and 1.0 neutral filter. Samples are diluted in TBSET prior to being loaded onto the FACS. Particles were first gated using side scatter and forward scatter, followed by gating using the presence or absence of the fluoresceine (FAM) fluorophore. FAM signal was identified using a 488 nm laser and a 505LP optical filter (BD Biosciences). An emulsion was defined as positive if it lies within a user-defined fluorescence range. The number of positive particles was recorded by the FACS Aria II and divided by the total number of droplets processed.

2.5 | Microfluidic sorting

Particles recovered from ddPCR reaction were mixed together with 300 μl of HFE-7500 oil supplemented with 5% w/w PFPE-PEG-PFPE surfactant (008-Fluoro-surfactant, RAN Biotechnologies) and enough Triton X-100 for a final concentration of 0.5% v/v in a 1.7-ml Eppendorf tube by tapping. The mixture is agitated at 3500 rpm for 20 s with a vortex (VWR) to reform the emulsion. The emulsion was allowed to settle for 1 min before 150 μl of the bottom oil phase was removed and replaced with fresh HFE-7500 oil supplemented with 5% w/w PFPE-PEG-PFPE surfactant. The tube was gently inverted several times to mix. Oil replacement was repeated three to five times or until most small satellite droplets that were generated from the PTE emulsification process[29] had been removed. The sample was injected into the microfluidic droplet sorter at a flow rate of 50 μl h^{-1}. The flow rates of spacer and bias oil were both 1000 μl h^{-1}. Both used HFE 7500 with 0.1% surfactant

loaded into 10 ml syringes. A 10 ml syringe connected to the waste channel outlet was set to constantly withdraw with a flow rate of –1000 μl h^{-1}. The electrode and moat channels were filled with 2 M NaCl solution.[35] The droplet fluorescence was excited with a 473 nm laser (CNI lasers) and a custom LabVIEW code (available at GitHub: https://github.com/AbateLab/sorter-code) detects the fluorescence signal in real time. Droplets having a fluorescent intensity within the user-defined range trigger a 40 kHz, 1 kV output pulse to the electrode that leads to droplet recovery.[36] A total of 10,000 droplets were collected for the downstream Illumina sequencing step. 1*H*,1*H*,2*H*,2*H*-Perfluoro-1-octanol (final concentration 20% v/v, SigmaAldrich) and 10 μl water was added to the droplets and then mixed to break emulsion.[32] The tube was centrifuged briefly and the aqueous droplet floating on top was transferred to a new clean tube.

2.6 | DNA sequencing and data analysis

Sorted droplets were used for library preparation with the Nextera XT library kit (Illumina). Sequencing library quality was assayed by Bioanalyzer (Agilent) using a High Sensitivity DNA Assay. Sequencing was performed with a MiSeq sequencer (Illumina). Reads were mapped to *E. coli* reference genome using Bowtie2.[37] Genome coverage at each position was calculated using SAMtools.[38] Reads were de novo assembled using SPAdes with default parameters.[39] Assembly results were evaluated by Quast.[40]

3 | RESULTS AND DISCUSSION

3.1 | Microfluidic-free NAC

The first step in NAC usually conducted with microfluidics is encapsulation of the cell suspension into monodispersed droplets for PCR detection. Recently, we demonstrated that PTE can encapsulate cells in monodispersed droplets with vortexing, and that PCR can be performed in the resultant emulsions to detect target nucleic acids.[29] To implement this approach for NAC (Table S1, Supporting Information), we use templating hydrogels to encapsulate the cell suspension and PCR reagents in a monodispersed emulsion by vortexing (Figure 1A). In the PTE process, droplets form spontaneously upon injection of shear energy, initially comprising large droplets with many particles and cells and, as emulsification progresses, small droplets with a single particle and volume of sample encapsulated as a shell (Figure 1B). Once this size is achieved, further emulsification is inhibited because it requires fragmenting the solid particles. The cell encapsulation process takes ≈1 min and cells are loaded randomly in the shells in accordance with Poisson statistics, just as in microfluidic-made emulsions.[41] The hydrogel particles are > 95% aqueous solution; due to their porosity, small molecules like PCR reagent and oligos, can freely diffuse through them while macromolecules, like genomic DNA, are excluded, remaining in the aqueous shell surrounding the particles (Figure 1B). Upon heating above 60°C, the agarose shell liquifies, mixing with the aqueous portion of the droplet; after cooling, the genome of the cell is captured in the resolidified agarose matrix and the particles can be redispersed in an aqueous phase while retaining the genomic material. In many cases, the sample can be directly thermocycled for detection.[42] However, if necessary, the solidified particles with entrapped cells can be soaked in a lysis cocktail that includes hydrolases and proteases to liberate the DNA.[43] After the lysis, inhibitory factors

like proteinase K can be washed out by buffer exchanges prior to re-emulsifying the particles for PCR. Post thermal cycling, particles containing target cells have fluorescent cores, while ones without remain dim (Figure 1C). To recover the genomes of the positive cells, we sort the particles (Figure 1D) and recover the genomes by melting the agarose, and prepare them for sequencing (Section 2, Figure 1E).

The second step of NAC that usually requires microfluidics is droplet sorting.[27] Previously, we showed NAC droplets could be sorted with FACS by converting them into double emulsions suspended in an aqueous carrier phase;[28] the double emulsions retain the fluorescent signal of the PCR reaction, allowing positive sorting. However, a drawback of this method is that double emulsions are incompatible with bulk washing, which limits flexibility. While this process might be modifiable to enable microfluidic-free NAC, a simpler strategy is to tether the PCR amplicons to the beads, then redisperse them into FACS-compatible carrier phase, and sort them directly. To accomplish this, we functionalize the polyacrylamide cores with a capture oligo nucleotide that yields tethered fluorescent amplicon products after PCR (Figure 2A). In this implementation, the beads (Figure 2A, *i.*) are emulsified with a PCR mix that contains a forward primer with a capture-tail and reverse primer with a conjugated fluorophore. The result is particles encased in a fluorescent solution (Figure 2A, *ii.*). Interspersed throughout the solution of encapsulated particles are also smaller satellite droplets formed from the PTE process. These smaller droplets will be eventually cleaned out when the hydrogel particles are recovered and, thus, do not interfere with future steps.[29] Thermocycling attaches a subset of the fluorophore-labeled primers onto the bead using the target amplicon as a splint (Figure 2A, *iii.*). Because of the excess primer, the change is not visible at this stage. Finally, the emulsion is broken to wash away unbound primers and reveal either fluorescent cores representing positive particles or dim ones indicative of negative particles (Figure 2A, *iv.*). The recovered dual-layer particles can then be suspended in a FACS-compatible carrier solution and differentiated by sorting.

To ensure that the cell's genome remains captured in the agarose, we modify the PCR denaturation temperature from a typical 95 to 87°C; this mitigates thermally induced fragmentation of DNA,[44,45] thereby retaining intact genomes within the agarose shells. To confirm the specificity and accuracy of this modified ddPCR assay, we perform a dilution series with different target concentrations, detecting bright droplets as expected for the conditions (Figure 2B). The estimated target concentration follows the expectation based on Poisson loading over ≈3 decades, typical of a ddPCR assay (Figure 2C). While we use standard PCR to generate the signal, other amplification methods like Loop-mediated isothermal amplification (LAMP) or recombinase polymerase amplification (RPA) are compatible.[46,47]

3.2 | Sorting PTE-NAC particles

To demonstrate the ability to isolate specific cells for sequencing using the PTE-NAC particles, we apply the workflow to a suspension of *E. coli* using genome-targeting primers (Section 2). We first sorted particles obtained after ddPCR using FACS (Figure 3A) and gating on scattering and fluorescence. Within the scatter value range indicative of the PTE-NAC particles (Figure 3B, *left*), we observe the expected bimodal fluorescence distribution

of positive and negative PCR populations (Figure 3B, *right*). The observed percent positive rate matches the expected input concentration of *E. coli* (200 copies per μl) predicted by the droplet encapsulation rate. Setting a fluorescence gate allows us to sort the positive droplets, yielding a recovery rate of ≈40% of anticipated positive hydrogels. This yield is typical for hydrogels of this size (50 μm diameter) with a flow cytometer, which is optimized for cells that are generally smaller (≈20 μm). If a higher yield is desired, several parameters can be optimized, including using smaller hydrogels and optimizing the timing of the sort delay, which has been shown to increase yield of recovered double emulsions of comparable size.[48]

PTE-NAC particles can also be sorted by other means if desired. This is especially important when sorted droplets must be sequenced and carry over DNA from the FACS machine can contaminate the sample.[49–51] For example, microfluidics sorters can provide similar speed, [52] with better yields. Moreover, because a fresh microfluidic chip is used for a single sort, the recovered particles are free of contaminating DNA that would otherwise interfere with the sequencing of recovered genomes. To illustrate such versatility, we also sort the particles with a droplet microfluidic sorter (Figure 4A). The particles are introduced into the device as a dense hydrogel pack,[53] encapsulated into droplets, and sorted based on fluorescence via dielectrophoresis. We use the concentric dielectrophoretic sorting geometry because it is robust and fast;[54] when gating by size and fluorescence (Figure 4B), this allows a sort rate of 40 kHz and yield of 95%, exceeding results of the flow cytometer.

3.3 | Genome recovery and sequencing

Using the PTE-NAC workflow, we recovered 10,000 fluorescence-positive particles and processed the recovered material for sequencing (Section 2). Although typical short-read Next Generation Sequencing library preparation recommends at least ≈1 ng of input DNA, [55] which amounts to ≈211,000 *E. coli* genomes,[56,57] lower input libraries measured in picograms have also been achieved.[58] After sequencing, we first quantify the results by aligning the raw reads against the *E. coli* genome. As expected for an approach without pre-sequencing whole genome amplification, we observe unbiased coverage across the genome showing a mean relative coverage of ≈1 (Figure 5A). To further assess the quality of the data, we de novo assemble the short reads into longer length contigs and plot the cumulative length distribution (Figure 5B) and contig size distribution (Figure 5C) (Table S2, Supporting Information). Both metrics demonstrate a healthy population of long, quality assemblies even at a total sequencing coverage of 1. These results demonstrate that PTE-NAC is an effective means by which to recover high quality genome sequence data from cells of interest.

4 | CONCLUSION

PTE provides an effective, microfluidic-free approach for isolating genomes of interest from a mixed suspension based on sequence motifs. By exploiting dual-layered hydrogels, robust detection of target cells can be accomplished while preserving and physically linking the cell genome to the fluorescent PCR signal, allowing isolation by FACS. The recovered, unamplified material is compatible with common library preparation and can be sequenced

to deliver high quality genomes with even coverage and long de novo assembled contigs. Moreover, removal of microfluidics from the workflow affords numerous benefits, including allowing standard laboratory equipment and methods and requiring limited expertise. Since no microfluidic devices are used, reagents and samples need not be transferred into microfluidic devices, allowing processing in well plates with multipipette or robotic fluid handling, for efficient and cost-effective sample processing. Additionally, semipermeable hydrogels allow washing with a variety of reagents, affording flexibility for optimizing cell lysis and PCR detection.[43,59] This is critical when applying NAC to microbial samples that often require harsh lysis procedures incompatible with droplet methods.[43] Lastly, while we have utilized hydrogels labeled with constant capture primers, the polyacrylamide cores are chemically identical to ones used in single cell workflows in which they are functionalized with barcode sequences upstream of the capture sequence.[60,61] This holds potential for implementing a variety of barcode-based sequencing strategies into NAC, to acquire additional single cell information, including protein (Ab-seq),[62] mRNA (e.g., Drop-seq),[60] DNA (e.g., SiC-seq, ATAC-seq),[43,63] and multiomic measurements (e.g., CITE-seq, DAb-seq).[64–66] These attributes make PTE-NAC a powerful strategy for isolating specific cells, viruses, or DNA sequences of interest from heterogenous suspensions, opening up unique opportunities in the characterization of understudied microbes in ecological and microbiome samples,[3] isolation of genomic islands for cell engineering and genetic disorders,[17,25] and deep characterization of disease causing genomic alterations in human cells, including HIV and cancer.[17,18]

Supplementary Material

Refer to Web version on PubMed Central for supplementary material.

ACKNOWLEDGEMENTS

This work was supported by the Chan Zuckerberg Biohub and the National Institutes of Health (NIH) (Grant No. R01-EB019453-01, DP2-AR068129-01, & R01-HG008978).

DATA AVAILABILITY STATEMENT

The data that support the findings of this study are available from the corresponding author upon reasonable request.

Abbreviations:

PCR	polymerase chain reaction
NAC	nucleic acid cytometry
PTE	particle-templated emulsification
FACS	fluorescence-activated cell sorting

REFERENCES

1. Habermann AC, Gutierrez AJ, Bui LT, Yahn SL, Winters NI, Calvi CL, Peter L, Chung M-I, Taylor CJ, Jetter C, Raju L, Roberson J, Ding G, Wood L, Sucre JMS, Richmond BW, Serezani AP, McDonnell WJ, Mallal SB, ... Kropski JA (2020). Singlecell RNA sequencing reveals profibrotic roles of distinct epithelial and mesenchymal lineages in pulmonary fibrosis. Science Advances, 6(28), eaba1972.
2. Bhaduri A, Di Lullo E, Jung D, Müller S, Crouch EE, Espinosa CS, Ozawa T, Alvarado B, Spatazza J, Cadwell CR, Wilkins G, Velmeshev D, Liu SJ, Malatesta M, Andrews MG, Mostajo-Radji MA, Huang EJ, Nowakowski TJ, Lim DA, ... Kriegstein AR (2020). Outer radial glia-like cancer stem cells contribute to heterogeneity of glioblastoma. Cell Stem Cell, 26(1), 48–63.e6. [PubMed: 31901251]
3. Richards TA, Massana R, Pagliara S, & Hall N (2019). Single cell ecology. Philosophical Transactions of the Royal Society B: Biological Sciences, 374(1786), 20190076.
4. Regev A, Teichmann SA, Lander ES, Amit I, Benoist C, Birney E, Bodenmiller B, Campbell P, Carninci P, Clatworthy M, Clevers H, Deplancke B, Dunham I, Eberwine J, Eils R, Enard W, Farmer A, Fugger L, Göttgens B, ... Human Cell Atlas Meeting Participants. (2017). The human cell atlas. ELife, 6, e27041.
5. Iqbal MM, Hurgobin B, Holme AL, Appels R, & Kaur P (2020). Status and potential of single-cell transcriptomics for understanding plant development and functional biology. Cytometry, *Part A*, 97(10), 997–1006. [PubMed: 32713117]
6. Delgado-Baquerizo M, Oliverio AM, Brewer TE, Benavent-González A, Eldridge DJ, Bardgett RD, Maestre FT, Singh BK, & Fierer N (2018). A global atlas of the dominant bacteria found in soil. Science (New York, N.Y.), 359(6373), 320–325.
7. Berardi AC, Wang A, Levine JD, Lopez P, & Scadden DT (1995). Functional isolation and characterization of human hematopoietic stem cells. Science, 267(5194), 104–108. [PubMed: 7528940]
8. Hodge RD, Miller JA, Novotny M, Kalmbach BE, Ting JT, Bakken TE, Aevermann BD, Barkan ER, Berkowitz-Cerasano ML, Cobbs C, Diez-Fuertes F, Ding S-L, McCorrison J, Schork NJ, Shehata SI, Smith KA, Sunkin SM, Tran DN, Venepally P, ... Lein ES (2020). Transcriptomic evidence that von Economo neurons are regionally specialized extratelencephalic-projecting excitatory neurons. Nature Communication, 11(1), 1172.
9. Miltenyi S, Müller W, Weichel W, & Radbruch A (1990). High gradient magnetic cell separation with MACS. Cytometry, 11(2), 231–238. [PubMed: 1690625]
10. Batani G, Bayer K, Böge J, Hentschel U, & Thomas T (2019). Fluorescence in situ hybridization (FISH) and cell sorting of living bacteria. Science Reports, 9(1), 18618.
11. Amamoto R, Garcia MD, West ER, Choi J, Lapan SW, Lane EA, Perrimon N, & Cepko CL (2019). Probe-Seq enables transcriptional profiling of specific cell types from heterogeneous tissue by RNA-based isolation. ELife, 8, e51452.
12. Larsson HM, Lee ST, Roccio M, Velluto D, Lutolf MP, Frey P, & Hubbell JA (2012). Sorting live stem cells based on Sox2 mRNA expression. Plos One, 7(11), e49874.
13. Herzenberg LA, De Rosa SC, & Herzenberg LA (2000). Monoclonal antibodies and the FACS: Complementary tools for immunobiology and medicine. Immunology Today, 21(8), 383–390. [PubMed: 10916141]
14. Meyfour A, Pahlavan S, Mirzaei M, Krijgsveld J, Baharvand H, & Salekdeh GH (2021). The quest of cell surface markers for stem cell therapy. Cellular and Molecular Life Sciences: CMLS, 78(2), 469–495. [PubMed: 32710154]
15. Close DW, Ferrara F, Dichosa AEK, Kumar S, Daughton AR, Daligault HE, Reitenga KG, Velappan N, Sanchez TC, Iyer S, Kiss C, Han CS, & Bradbury ARM (2013). Using phage display selected antibodies to dissect microbiomes for complete de novo genome sequencing of low abundance microbes. BMC Microbiology, 13, 270. [PubMed: 24279426]
16. Pellegrino M, Sciambi A, Yates JL, Mast JD, Silver C, & Eastburn DJ (2016). RNA-Seq following PCR-based sorting reveals rare cell transcriptional signatures. Bmc Genomics [Electronic Resource], 17(1), 361.

17. Stieglitz E, Troup C, Gelston L, Haliburton JR, Chow E, Yu K, Akutagawa J, Taylor-Weiner A, Liu YL, Wang Y-D, Beckman K, Emanuel P, Benjamin B, Abate AR, Gerbing R, Alonzo T, & Loh M (2015). Subclonal mutations in SETBP1 confer a poor prognosis in juvenile myelomonocytic leukemia. Blood, 125(3), 516–524. [PubMed: 25395418]
18. Clark IC, Delley CL, Sun C, Thakur R, Stott SL, Thaploo S, Li Z, Quintana FJ, & Abate AR (2020). Targeted single-cell RNA and DNA sequencing with fluorescence-activated droplet merger. Analytical Chemistry, 92(21), 14616–14623. [PubMed: 33049138]
19. Jiang D, Ni C, Tang W, Huang D, & Xiang N (2021). Inertial microfluidics in contraction-expansion microchannels: A review. Biomicrofluidics, 15(4), 041501.
20. Tang W, Zhu S, Jiang D, Zhu L, Yang J, & Xiang N (2020). Channel innovations for inertial microfluidics. Lab on a Chip, 20(19), 3485–3502. [PubMed: 32910129]
21. Xiang N, & Ni Z (2021). Electricity-free hand-held inertial microfluidic sorter for size-based cell sorting. Talanta, 235, 122807. 10.1016/j.talanta.2021.122807.
22. Zhu S, Jiang F, Han Y, Xiang N, & Ni Z (2020). Microfluidics for label-free sorting of rare circulating tumor cells. Analyst, 145(22), 7103–7124. [PubMed: 33001061]
23. Clark IC, & Abate AR (2017). Finding a helix in a haystack: Nucleic acid cytometry with droplet microfluidics. Lab on a Chip, 17(12), 2032–2045. [PubMed: 28540956]
24. Joensson HN, Samuels ML, Brouzes ER, Medkova M, Uhlén M, Link DR, & Andersson-Svahn H (2009). Detection and analysis of low-abundance cell-surface biomarkers using enzymatic amplification in microfluidic droplets. Angewandte Chemie (International Ed. in English), 48(14), 2518–2521. [PubMed: 19235824]
25. Lim SW, Lance ST, Stedman KM, & Abate AR (2017). PCR-activated cell sorting as a general, cultivation-free method for high-throughput identification and enrichment of virus hosts. Journal of Virological Methods, 242, 14–21. [PubMed: 28042018]
26. Lance ST, Sukovich DJ, Stedman KM, & Abate AR (2016). Peering below the diffraction limit: Robust and specific sorting of viruses with flow cytometry. Virology Journal, 13(1).
27. Eastburn DJ, Huang Y, Pellegrino M, Sciambi A, Ptáček LJ, & Abate AR (2015). Microfluidic droplet enrichment for targeted sequencing. Nucleic Acids Research, 43(13), e86–e86. [PubMed: 25873629]
28. Sukovich DJ, Lance ST, & Abate AR (2017). Sequence specific sorting of DNA molecules with FACS using 3dPCR. Science Reports, 7(1), 39385.
29. Hatori MN, Kim SC, & Abate AR (2018). Particle-templated emulsification for microfluidics-free digital biology. Analytical Chemistry, 90(16), 9813–9820. [PubMed: 30033717]
30. Kumaresan P, Yang CJ, Cronier SA, Blazej RG, & Mathies RA (2008). High-throughput single copy DNA amplification and cell analysis in engineered nanoliter droplets. Analytical Chemistry, 80(10), 3522–3529. [PubMed: 18410131]
31. Yan Z, Clark IC, & Abate AR (2017). Rapid Encapsulation of cell and polymer solutions with bubble-triggered droplet generation. Macromolecular Chemistry and Physics, 218(2), 1600297.
32. Mazutis L, Araghi AF, Miller OJ, Baret J-C, Frenz L, Janoshazi A, Taly V, Miller BJ, Hutchison JB, Link D, Griffiths AD, & Ryckelynck M (2009). Droplet-based microfluidic systems for high-throughput single DNA molecule isothermal amplification and analysis. Analytical Chemistry, 81(12), 4813–4821. [PubMed: 19518143]
33. Zhang Z, Yang X, Meng L, Liu F, Shen C, & Yang W (2009). Enhanced amplification of GC-rich DNA with two organic reagents. Biotechniques, 47(3), 775–779. [PubMed: 19852763]
34. Sidore AM, Lan F, Lim SW, & Abate AR (2016). Enhanced sequencing coverage with digital droplet multiple displacement amplification. Nucleic acids research, 44(7), e66. [PubMed: 26704978]
35. Sciambi A, & Abate AR (2014). Generating electric fields in PDMS microfluidic devices with salt water electrodes. Lab on a Chip, 14(15), 2605–2609. [PubMed: 24671446]
36. Cole RH, Gartner ZJ, & Abate AR (2016). Multicolor fluorescence detection for droplet microfluidics using optical fibers. Journal of Visualized Experiments, 111, 54010.
37. Langmead B, & Salzberg SL (2012). Fast gapped-read alignment with Bowtie 2. Nature Methods, 9(4), 357–359. [PubMed: 22388286]

38. Li H, Handsaker B, Wysoker A, Fennell T, Ruan J, Homer N, Marth G, Abecasis G, Durbin R, & 1000 Genome Project Data Processing Subgroup. (2009). The sequence alignment/Map format and SAMtools. Bioinformatics (Oxford, England), 25(16), 2078–2079.
39. Bankevich A, Nurk S, Antipov D, Gurevich AA, Dvorkin M, Kulikov AS, Lesin VM, Nikolenko SI, Pham S, Prjibelski AD, Pyshkin AV, Sirotkin AV, Vyahhi N, Tesler G, Alekseyev MA, & Pevzner PA (2012). SPAdes: A new genome assembly algorithm and its applications to single-cell sequencing. Journal of Computational Biology, 19(5), 455–477. [PubMed: 22506599]
40. Gurevich A, Saveliev V, Vyahhi N, & Tesler G (2013). QUAST: Quality assessment tool for genome assemblies. Bioinformatics (Oxford, England), 29(8), 1072–1075.
41. Collins DJ, Neild A, deMello A, Liu A-Q, & Ai Y (2015). The Poisson distribution and beyond: Methods for microfluidic droplet production and single cell encapsulation. Lab on a Chip, 15(17), 3439–3459. [PubMed: 26226550]
42. Fode-Vaughan KA, Wimpee CF, Remsen CC, & Collins ML (2001). Detection of bacteria in environmental samples by direct PCR without DNA extraction. Biotechniques, 31(3), 598, 600, 602–604, passim. [PubMed: 11570503]
43. Lan F, Demaree B, Ahmed N, & Abate AR (2017). Single-cell genome sequencing at ultra-high-throughput with microfluidic droplet barcoding. Nature Biotechnology, 35(7), 640–646.
44. Douglas A, & Atchison B (1993). Degradation of DNA during the denaturation step of PCR. Genome Research, 3(2), 133–134.
45. Gustafson CE, Alm RA, & Trust TJ (1993). Effect of heat denaturation of target DNA on the PCR amplification. Gene, 123(2), 241–244. [PubMed: 8428664]
46. Schuler F, Siber C, Hin S, Wadle S, Paust N, Zengerle R, & von Stetten F (2016). Digital droplet LAMP as a microfluidic app on standard laboratory devices. Analytical Methods, 8(13), 2750–2755.
47. Schuler F, Schwemmer F, Trotter M, Wadle S, Zengerle R, von Stetten F, & Paust N (2015). Centrifugal step emulsification applied for absolute quantification of nucleic acids by digital droplet RPA. Lab on a Chip, 15(13), 2759–2766. [PubMed: 25947077]
48. Brower KK, Carswell-Crumpton C, Klemm S, Cruz B, Kim G, Calhoun SGK, Nichols L, & Fordyce PM (2020). Double emulsion flow cytometry with high-throughput single droplet isolation and nucleic acid recovery. Lab on a Chip, 20(12), 2062–2074. [PubMed: 32417874]
49. Imamura H, Monsieurs P, Jara M, Sanders M, Maes I, Vanaerschot M, Berriman M, Cotton JA, Dujardin J-C, & Domagalska MA (2020). Evaluation of whole genome amplification and bioinformatic methods for the characterization of Leishmania genomes at a single cell level. Science Reports, 10(1), 15043.
50. Džunková M, Moya A, Chen X, Kelly C, & D'Auria G (2020). Detection of mixed-strain infections by FACS and ultra-low input genome sequencing. Gut Microbes, 11(3), 305–309. [PubMed: 30289342]
51. Wiegand S, Dam HT, Riba J, Vollmers J, & Kaster A-K (2021). Printing microbial dark matter: Using single cell dispensing and genomics to investigate the patescibacteria/candidate phyla radiation. Frontiers in Microbiology, 12, 635506.
52. Sciambi A, & Abate AR (2015). Accurate microfluidic sorting of droplets at 30 kHz. Lab on a Chip, 15(1), 47–51. [PubMed: 25352174]
53. Abate AR, Chen C-H, Agresti JJ, & Weitz DA (2009). Beating Poisson encapsulation statistics using close-packed ordering. Lab on a Chip, 9(18), 2628. [PubMed: 19704976]
54. Clark IC, Thakur R, & Abate AR (2018). Concentric electrodes improve microfluidic droplet sorting. Lab on a Chip, 18(5), 710–713. 10.1039/C7LC01242J. [PubMed: 29383336]
55. Bronner IF, & Quail MA (2019). Best practices for illumina library preparation. Current Protocols in Human Genetics, 102(1), e86. [PubMed: 31216112]
56. Blattner FR (1997). The complete genome sequence of *Escherichia coli* K-12. Science, 277(5331), 1453–1462. [PubMed: 9278503]
57. Dolezel J, Bartos J, Voglmayr H, & Greilhuber J (2003). Nuclear DNA content and genome size of trout and human. Cytometry, 51A(2), 127–128.

58. Rinke C, Low S, Woodcroft BJ, Raina J-B, Skarshewski A, Le XH, Butler MK, Stocker R, Seymour J, Tyson GW, & Hugenholtz P (2016). Validation of picogram- and femtogram-input DNA libraries for microscale metagenomics. PeerJ, 4, e2486. [PubMed: 27688978]

59. Zhu Y, Li J, Lin X, Huang X, & Hoffmann MR (2021). Single-cell phenotypic analysis and digital molecular detection linkable by a hydrogel bead-based platform. ACS Applied Bio Materials, 4(3), 2664–2674. 10.1021/acsabm.0c01615.

60. Macosko EZ, Basu A, Satija R, Nemesh J, Shekhar K, Goldman M, Tirosh I, Bialas AR, Kamitaki N, Martersteck EM, Trombetta JJ, Weitz DA, Sanes JR, Shalek AK, Regev A, & McCarroll SA (2015). Highly parallel genome-wide expression profiling of individual cells using nanoliter droplets. Cell, 161(5), 1202–1214. [PubMed: 26000488]

61. Klein AM, Mazutis L, Akartuna I, Tallapragada N, Veres A, Li V, Peshkin L, Weitz DA, & Kirschner MW (2015). Droplet barcoding for single-cell transcriptomics applied to embryonic stem cells. Cell, 161(5), 1187–1201. [PubMed: 26000487]

62. Shahi P, Kim SC, Haliburton JR, Gartner ZJ, & Abate AR (2017). Abseq: Ultrahigh-throughput single cell protein profiling with droplet microfluidic barcoding. Science Reports, 7(1), 44447.

63. Buenrostro JD, Giresi PG, Zaba LC, Chang HY, & Greenleaf WJ (2013). Transposition of native chromatin for fast and sensitive epigenomic profiling of open chromatin, DNA-binding proteins and nucleosome position. Nature Methods, 10(12), 1213–1218. [PubMed: 24097267]

64. Stoeckius M, Hafemeister C, Stephenson W, Houck-Loomis B, Chattopadhyay PK, Swerdlow H, Satija R, & Smibert P (2017). Simultaneous epitope and transcriptome measurement in single cells. Nature Methods, 14(9), 865–868. [PubMed: 28759029]

65. Demaree B, Delley CL, Vasudevan HN, Peretz CAC, Ruff D, Smith CC, & Abate AR (2021). Joint profiling of DNA and proteins in single cells to dissect genotype-phenotype associations in leukemia. Nature Communication, 12(1), 1583.

66. Nam AS, Kim K-T, Chaligne R, Izzo F, Ang C, Taylor J, Myers RM, Abu-Zeinah G, Brand R, Omans ND, Alonso A, Sheridan C, Mariani M, Dai X, Harrington E, Pastore A, Cubillos-Ruiz JR, Tam W, Hoffman R, ... Landau DA (2019). Somatic mutations and cell identity linked by genotyping of transcriptomes. Nature, 571(7765), 355–360. [PubMed: 31270458]

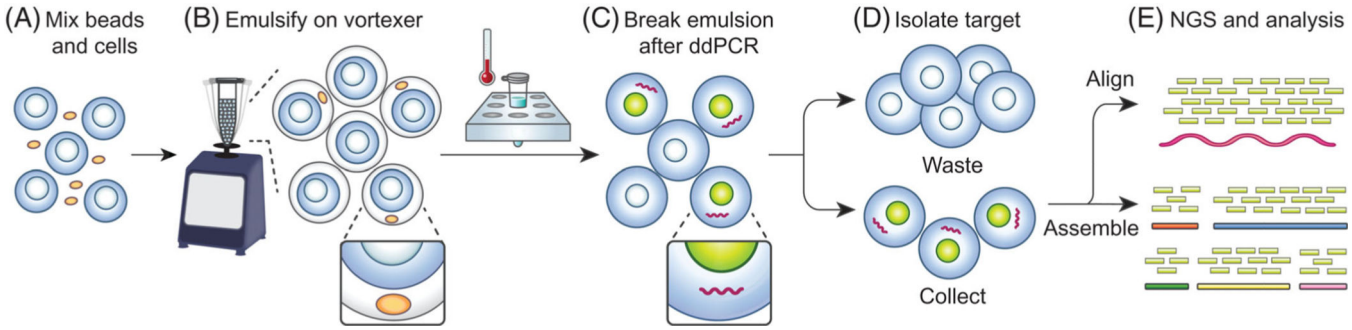

FIGURE 1.

Schematic of the PTE-NAC workflow. (A) Cell solution is combined with the dual layered PTE particles, consisting of a functionalized polyacrylamide core and agarose shell, and then (B) emulsified by vortexing. (C) After thermocycling, the emulsion is broken and (D) the hydrogels are isolated. Particles encapsulated with target cells become fluorescently labeled and capture the genome because of the thermocycling. (E) After sorting, the genome is recovered from hydrogel, any desired whole genome amplification is performed, and the sample is subjected to NGS. Reads are mapped to reference genome or assembled

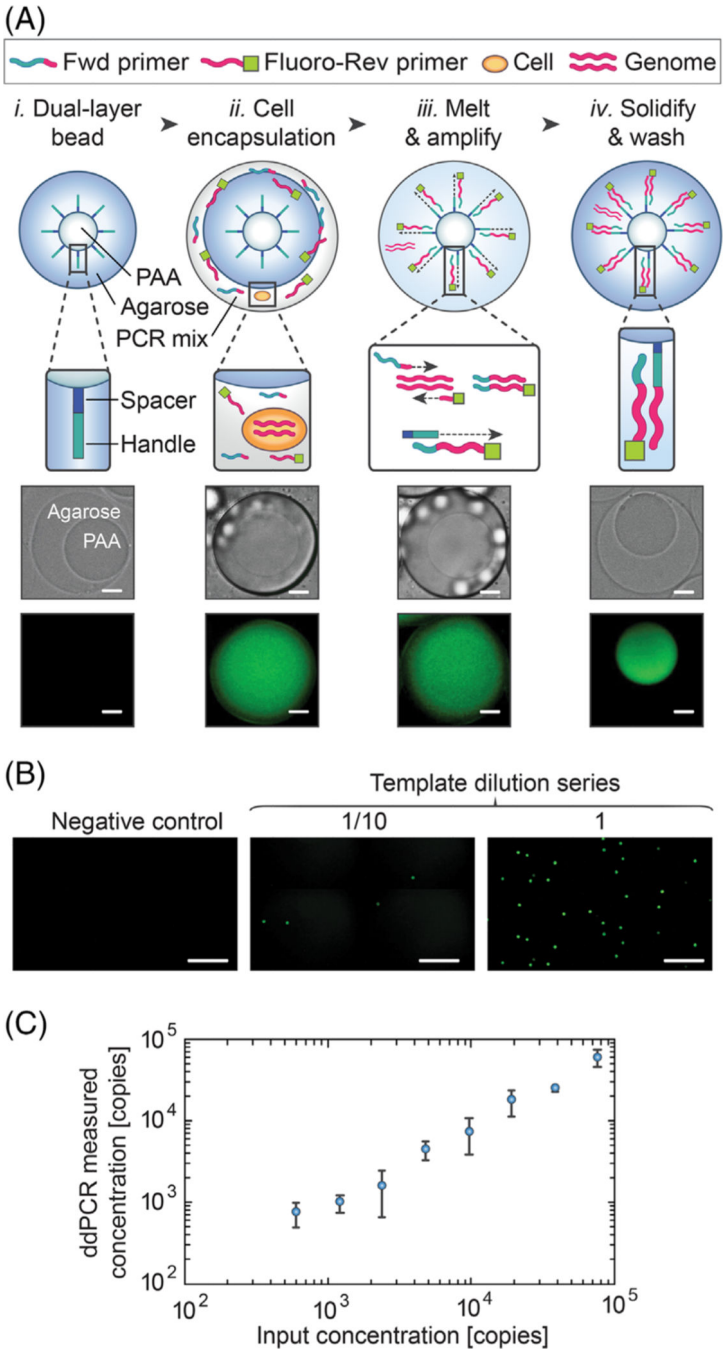

FIGURE 2.

Dual layered PTE particles become fluorescent after a productive ddPCR reaction when using a fluorophore-tagged primer. (A) Schematic with associated brightfield and fluorescence images of the different stages of the ddPCR detection process: *i.* dual layered PTE particles with a polyacrylamide (PAA) core and agarose shell that allow for the microfluidic-free generation of a monodisperse emulsion; *ii.* after vortexing, cells (not visible at the provided magnification) in solution are encapsulated within the thin aqueous phase filled with fluorescent primer and PCR mix surrounding each particle; *iii.* during

the PCR reaction, the agarose shell melts and the fluorophore-tagged primers are tethered onto the PAA particles; *iv.* at the end of thermocycling the agarose solidifies and captures the genome, allowing it to be retained with the fluorescently-tagged PAA core when the emulsion is broken to wash away the unbound primers. White spheres seen in the two center images are out-of-plane satellite droplets formed from the vortexing process. Scale bar represents 10 μm. (B) Fluorescence images of particle populations after amplification and demulsification from a template dilution series. Scale bar represents 400 μm. (C) Plot showing that fractions of observed fluorescence positive droplets correspond with the template concentration

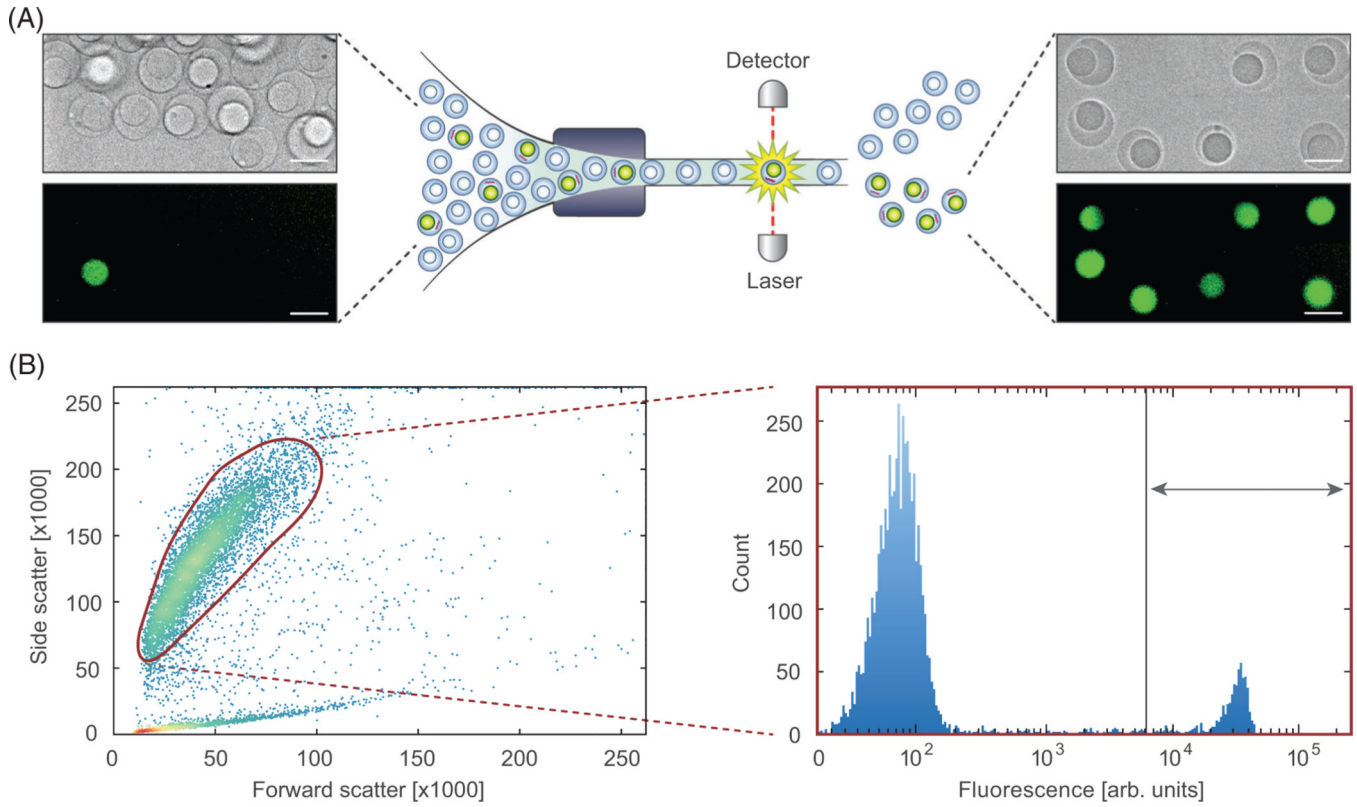

FIGURE 3.

Particles can be detected and sorted using FACS. (A) Schematic of FACS with images of washed particle solutions before and after sorting. Scale bar represents 50 μm. (B) Particle gating based on scattering (*left*) and fluorescence (*right*). Gated regions are represented by the red polygon and threshold line, respectively

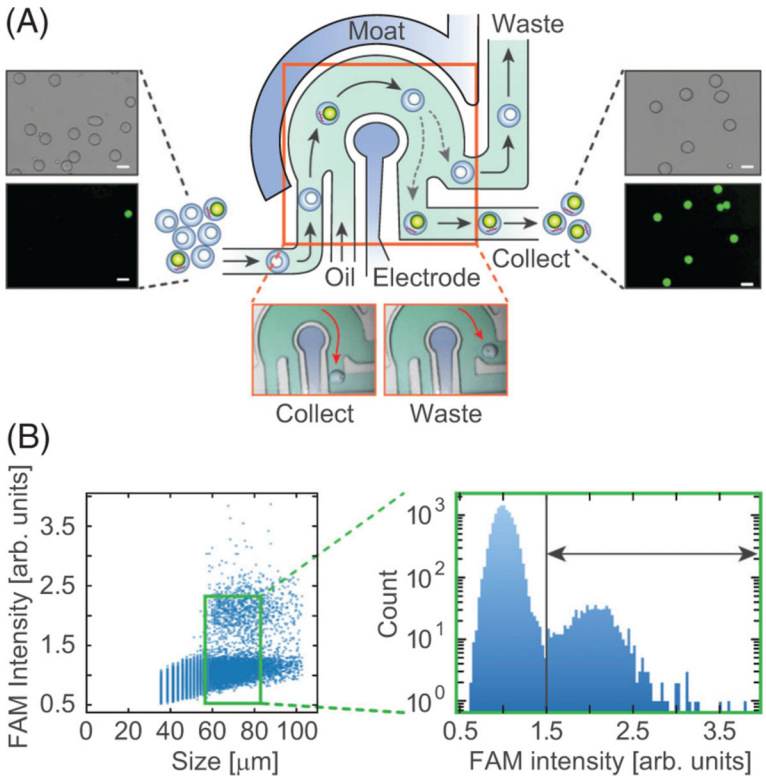

FIGURE 4.

Particles remain detectable and sortable on a microfluidic sorter. (A) Schematic of microfluidic sorter with images of washed particle solutions before and after sorting. Scale bar represents 50 μm. (B) Particle gating based on size (*left*) and fluorescence (FAM, *right*). Gated regions are represented by the green polygon and threshold line, respectively

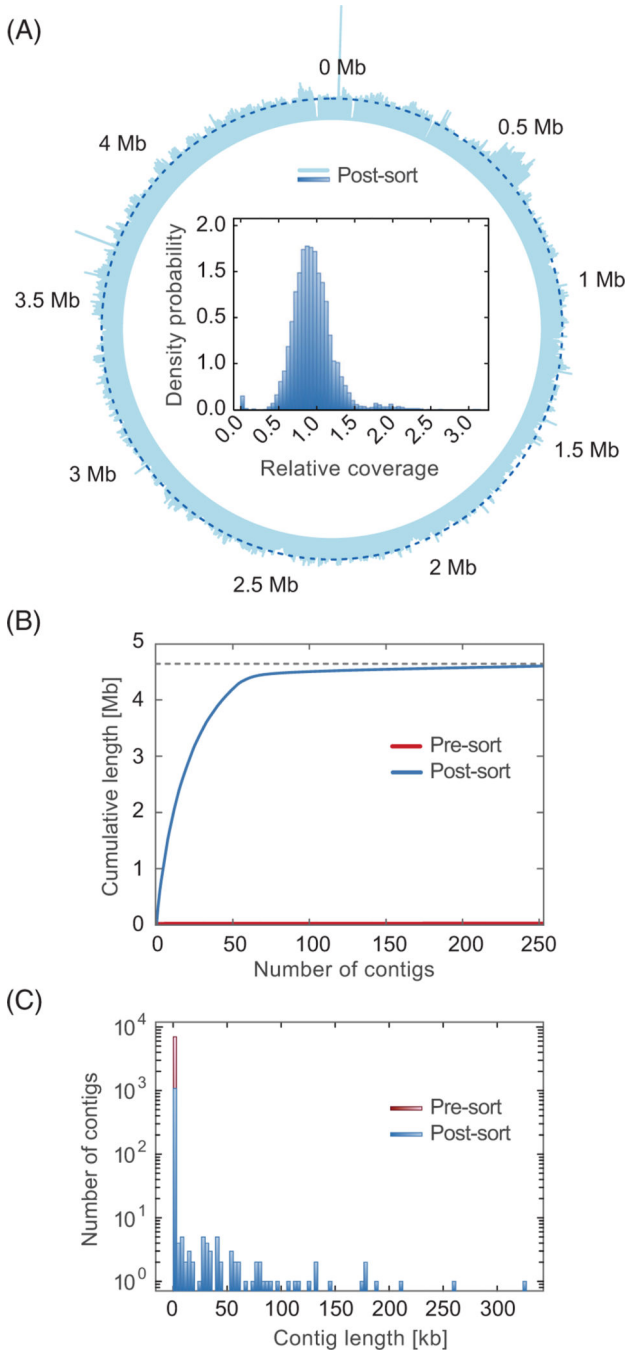

FIGURE 5.

Enriched genome sequencing is possible using PTE-NAC. (A) Circular graph of coverage. Dashed line represents average sequencing depth (43.65-fold). Inner histogram shows relative coverage probability. (B) Cumulative length plot and (C) contig length distribution histogram for de novo assembled contigs. Both pre-sorted and post-sorted sequenced populations consisted of 10,000 particles